Emergent Faces in Crystal Etching *†

Ted J. Hubbard‡
Erik K. Antonsson§
Engineering Design Research Laboratory
Division of Engineering and Applied Science
California Institute of Technology

January 25, 1995

Abstract

The time development of emergent faces in crystal etching is investigated. We present and discuss a novel computational approach, based on an intuitive geometrical derivation, for predicting an etched shape given an initial polygonal (mask) shape and a diagram of etch rate as a function of orientation. A two dimensional geometric model is derived which determines the etched shape as a function of time. The model is both intuitive and easy to implement manually or by computer. Because the model is intuitive in nature, some results can be obtained from only partial information. In addition, the model is a first step in the transition from analysis to design. Rather than predicting the etched shape for a given original shape, often what is desired is the original mask shape needed to produce a particular etched shape. This inversion process is carried out for some special cases. The concepts of equilibrium or eigen shapes (Eshapes), limit shapes, and time scaling are introduced. Model predictions are compared with experimental results. The extension from two dimensions to three is also presented.

1 Introduction

As the complexity of MEMS devices and the scope of MEMS applications increases, the need for good design, CAD, and modeling also increases. While design methods for VLSI are highly developed [1], they have primarily focused on surface micromachining of shallow rectangular shapes. The ability to represent and manipulate complex (mechanical) shapes to be fabricated in silicon remain primitive. This paper introduces a new method for modeling etching of single-crystalline silicon for

---

*Manuscript prepared for submission to the *IEEE/ASME Journal of Microelectromechanical Systems*

†Word Count: 4200 words.

‡Graduate Research Assistant

§Corresponding author: Associate Professor of Mechanical Engineering, Mail Code 104-44, Caltech, Pasadena, CA 91125, FAX: 818/568-2719, e-mail: erik@design.caltech.edu

arbitrarily complex MEMS fabrication, as a first step in developing comprehensive MEMS design methods approaching the level of development and automaticity in VLSI design.

One very common MEMS fabrication technique is the anisotropic etching of crystalline silicon. The anisotropy is utilized to create etched shapes of interest, and apparently arises because different crystal planes present different area densities of atoms and different surfaces which leads to different etch rates.

This type of etching can be described by an etch rate diagram which indicates etch rate as a function of the orientation of the surface to be etched within the crystal. While full three dimensional etch rate diagrams are generally not available for most etchants, some two dimensional etch rate diagrams have been obtained [2, 3]. The (100) plane etch rate diagrams for KOH and EDP are of the form given qualitatively by Figure 1. Note that the etching is slowest along the (111) family of planes and faster on the (011) family. However the modeling of anisotropic etching is not straightforward because certain faces may appear while others may disappear [4]. This chapter will examine the modeling of emergent faces in crystal etching.

1.1 Prior work

There are a number of methods for predicting the output shapes. The Wulff-Jaccodine method [5, 6] uses plane waves that propagate outwards at a rate given by the etch rate diagram. At each point on the initial surface, a tangent plane is moved outward a distance equal to the appropriate rate multiplied by the time. At sharp corners there is a geometrical test to determine if new planes appear. The final shape is the envelope of all these planes. Buser (*et al.*) [7] have developed a useful analysis tool called ASEP which can predict the output shape based on travelling planes. These results have been verified experimentally. However, their analysis is limited to a number of dominant plane families (111, 100, 110, 311) which tend to appear in crystal etching.

The slowness method [4] uses the inverse of the rate (the slowness) to calculate the trajectories of points or lines in the shape. The trajectory of a corner is given by a vector relation involving the slowness vectors of the two lines which form the corner. This relation states that the trajectory of the corner lies along the normal to the difference of the two line slowness vectors. The trajectories of the corners are then used to determine when lines disappear and the procedure is iterated to find the shape at any time. Sequin [4] has successfully used the slowness method to model changing shapes, although experimental verification is not included in that publication.

In this chapter I present a third, geometric model which combines some aspects of the two previous models, and various observations, to form a more complete and concise description of crystal etching. A comparison with previous work will be presented at the the end of the derivation. Linear models including the one presented here do not consider non-linear processes such as diffusion, however, such linear models do give accurate results where the effects of diffusion are small.

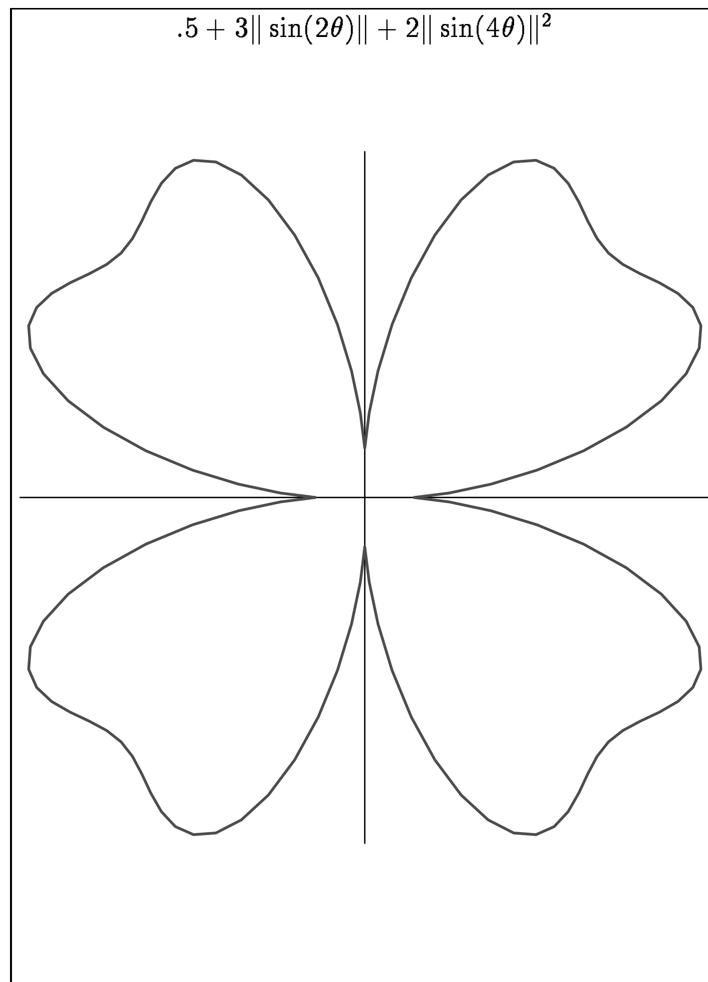

Figure 1: A qualitative example of an etch rate diagram. The formula for this rate in terms of angle θ is given above the figure. Etchants such as KOH and EDP have (100) etch rate diagrams which are very similar to the above figure.

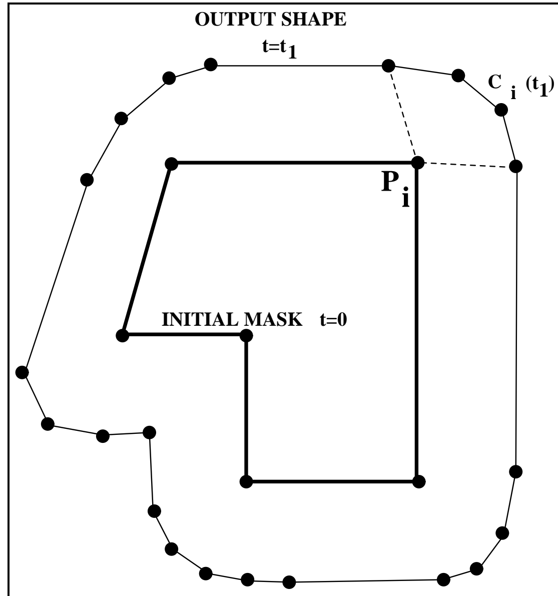

Figure 2: Evolution of corners.

2 Mathematical Derivation

2.1 Shapes

The fundamental process that we are modeling is one of applying an etch-resistant mask to portions of a wafer of silicon, and exposing the non-masked portions of the surface to an anisotropic etchant. Anisotropic etchant refers to etchants whose etching rate depend on orientation. The etchant removes silicon and creates a depression in the surface which grows both in the direction normal to the surface of the wafer (down), and also laterally. Because the etchants of interest are anisotropic, the rates at which material is removed in the various directions are different.

We model the mask and etched shapes as (arbitrarily complex) polygons, and therefore our model of the etching process must properly account for the behavior of the sides of the polygons (planes, or tangents in 2-D) and the corners. We model the corners as a polygonal approximation to a circular curve with an infinitesimal radius. Thus each corner contains a very large number of nearly coincident planes or tangents. Our model focuses on the evolution of these planes as the etching takes place, with particular attention paid to the corners (since all planes or tangents in the entire polygonal shape appear at the corners).

Consider an arbitrary initial polygon defined by a set of m vertices $\{P_i\}$; we wish to find its shape at a later time. At each t the vertex P_i is mapped to a set of points $\{C_{i_1}(t), ...C_{i_{N_i}}(t)\}$ and these points are connected to form a piecewise linear curve (See Figure 2). The key lies in determining the set of points C_i which model the evolving corner shapes.

2.2 Envelopes

The algorithm we have developed makes the following assumptions: The etch rate is independent of time, is a function of orientation only, and is given by an etch rate diagram.

In two dimensions, the x and y positions of a point define a vector [x,y] . A general vector is denoted by $\vec{V}$, its unit vector by $\hat{V}$ and its magnitude by V. If $\vec{V}$ is a function of some variable s, then $\vec{V}(s)$ is used. t is time.

Consider the region near a corner P_i as shown in Figure 3A: the perpendicular distance from a local tangent plane to a local initial corner position is $R(\theta) * t$, where $R(\theta)$ is the etch rate as a function of orientation and θ is the orientation of the tangent. We wish to find the envelope of tangents displaced a distance $R(\theta) * t$ from the initial corner position as shown in Figure 3A.

The new evolved corner will be defined by the envelope of displaced tangents that move out at rates dependent on their orientation.

In order to understand the complete envelope formed by all the tangents, let us first examine one of the points on the envelope formed by the intersection of two adjacent tangents as shown in Figure 3B.

Let $\vec{E}$ be the vector per unit time from the initial corner to the intersection of two adjacent local tangents. From Figure 3B we see that in the (R, θ) reference frame (denoted by superscript $\star$)

$$\vec{E}^{\star}(\theta) = \left[R, \frac{dR}{d\theta}\right] \tag{1}$$

Transforming to the initial reference frame using a rotation matrix, we obtain

$$\vec{E}(\theta) = \left[R(\theta), \frac{dR(\theta)}{d\theta}\right] \; ROT_{\theta} \tag{2}$$

where

$$ROT_{\theta} = \begin{bmatrix} \cos\theta & \sin\theta \\ -\sin\theta & \cos\theta \end{bmatrix} \tag{3}$$

Interestingly, Equation 1 also appears in the study of disk cams with flat-faced followers where the follower maintains tangential contact with the cam [8].

The local normal of the etch rate diagram is given by:

$$R_{\perp} = \left[1, -\frac{1}{R}\,\frac{dR}{d\theta}\right] \tag{4}$$

Thus $\vec{E}$ is the local normal of $R(\theta)$, (here denoted by $R_{\perp}$) multiplied by R then reflected about the R axis:

$$\vec{E}(\theta, t) = R \; R_{\perp} \begin{bmatrix} 1 & 0 \\ 0 & -1 \end{bmatrix} ROT_{\theta} \tag{5}$$

From Equation 4, it can be seen that the E differs from the etch rate diagram in that an individual point on the etch rate diagram at an angle θ is rotated in the θ direction an angle equal to the local derivative of the rate at that point with respect to θ.

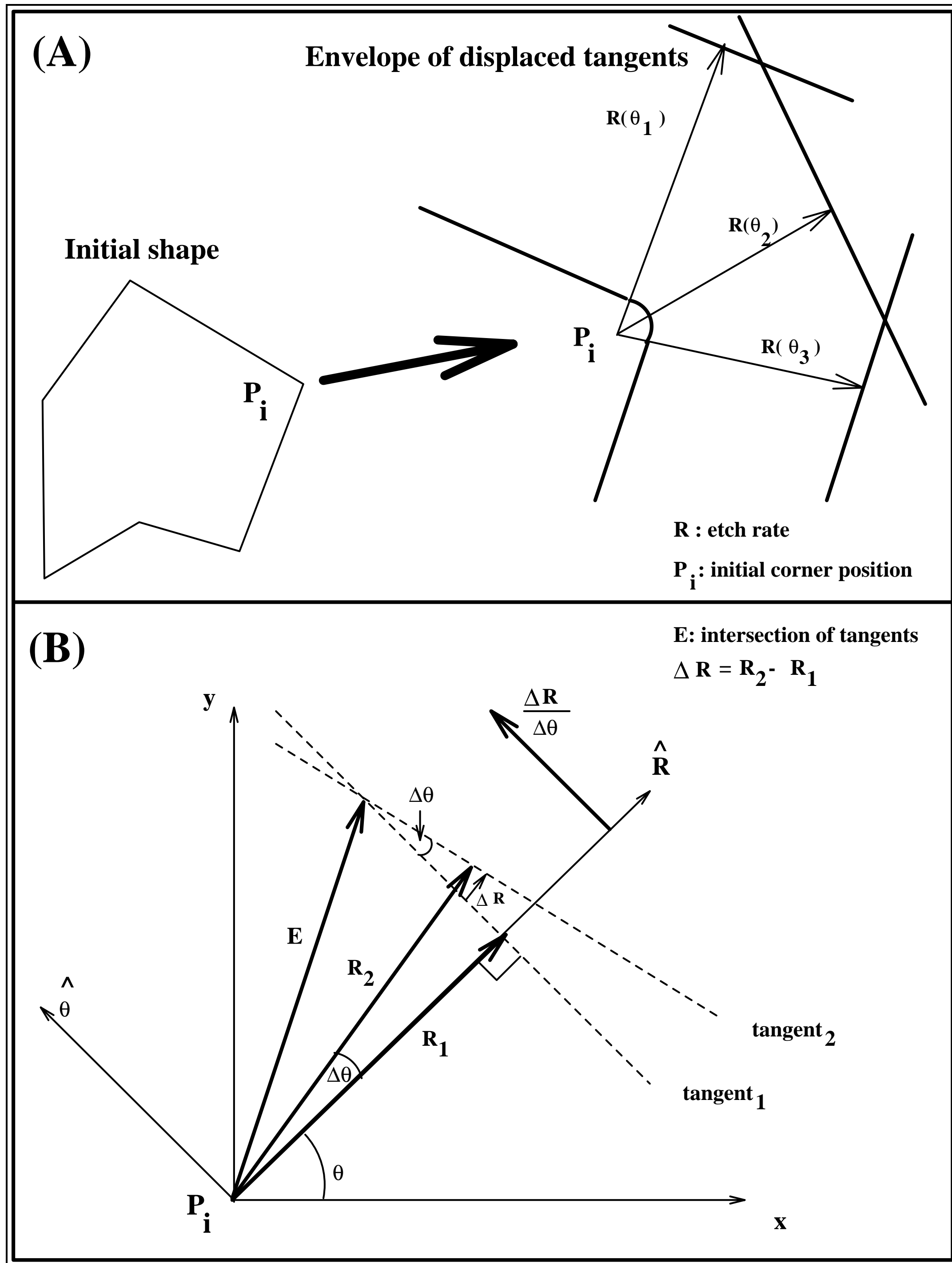

Figure 3: (A) Corner evolving to envelope of tangents. (B) Intersection of two adjacent tangents near a corner.

2.3 Eshapes

Plots of the of $E(\theta)$ that cover the entire range of θ are termed Eshapes (envelope, equilibrium, or eigen shapes). Because the complete Eshapes contain all possible envelopes, they also contain all possible evolving corners. The evolving corners (where the ith corner is denoted C_i as shown in Figure 2) are found by extracting a subset of the Eshape termed an Esection. If $(\theta_1)_i$ and $(\theta_2)_i$ are the angles of the two line segments forming the ith vertex, C_i is obtained from the section of the Eshape, $E(\theta)$, lying between $(\theta_1)_i$ and $(\theta_2)_i$. C_i may consist of from one to N_i points and the jth point is denoted C_{i_j}. For each corner, a set of points is taken from the Eshape region and this set is translated to the initial corner position and then scaled with time:

$$C_{i_j}(t) = \{P_i \; + t \; * \; E(\theta_{ij})\} \tag{6}$$

where the angle of the jth point in C_i is given by $\theta_{ij} = (\theta_1)_i + j * ((\theta_2)_i - \theta_1)/N_i$

The map $t \mapsto \{C_{i_1}(t), ...C_{i_{N_i}}(t)\}$ has the property:

$$\{C_{i_1}(\alpha t) - P_i, ...C_{i_{N_i}}(\alpha t) - P_i\} = \alpha\{C_{i_1}(t) - P_i, ...C_{i_{N_i}}(t) - P_i\}$$

Thus individual evolved corners obtained from the Eshape do linearly change size but do not change shape as a function of time (hence the name equilibrium).

The evolved shape S is given by a set of evolved corners $C_i(t)$ which themselves are a combination of the original polygon P and the Eshape E:

$$S(t) = \{C_1(t), C_2(t), ...C_m(t)\} \tag{7}$$

Figure 4 shows two hypothetical etch rate diagrams and the resulting Eshapes.

By differentiating E with respect to θ, we obtain the following test to determine the location of cusps in the Eshape,

$$\frac{d^2R(\theta)}{d\theta^2} + R(\theta) = 0 \tag{8}$$

If Equation 8 is satisfied by any θ, then the Eshape will be non-simple.

Eshapes and Esections will be examined further below.

2.4 Corners

There are two types of corners in two dimensions: convex and concave (see Figure 5). A square hole has 4 concave corners, while a triangular peg has 3 convex corners. The inside of a corner is taken to mean the region defined by an angle smaller than 180 degrees. For a convex corner, the inside is unetched, while the inside of a concave corner is etched.

To determine the shape of an etched corner at a later time, begin at each corner of the initial polygonal shape, and locate the two lines forming the corner. [1] The

[1] We approximate all shapes as arbitrarily complex polygons, hence the shapes are composed of straight line segments and corners. For a curve approximated with many chords, the line segments will be short, and the angle between them near 180 degrees.

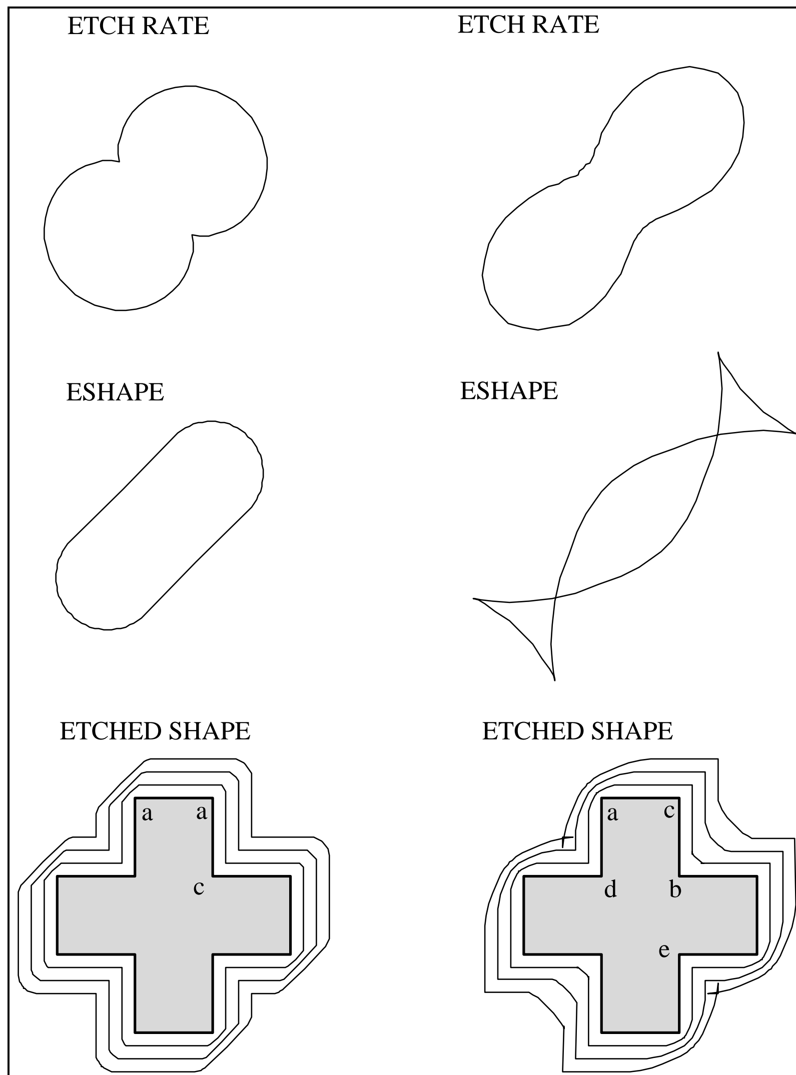

Figure 4: Hypothetical two dimensional etch rate diagram (top), corresponding Eshapes (center), and Etched shape (bottom). Note that the two etchants are not real etchants. The initial mask shape was the cross shaped hole shown at the bottom of the Figure.

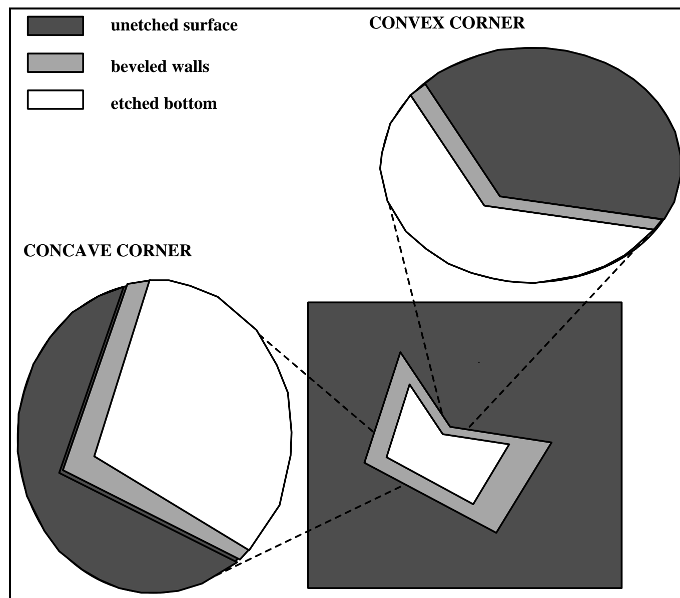

Figure 5: Definition of convex and concave corners.The unetched mask is dark, the etched bottom is light, and the beveled walls are grey.

appropriate Esection can be determined by finding points on the Eshape that are tangent to these two lines. The etched corner shape corresponds to the region of the Eshape between the two points of tangency. Figures 4 and 6 show the use of the Eshape method for predicting output corner shapes. Please note that hypothetical, asymmetrical, etchants have been used to demonstrate the model. The predictions for these figures are correct for these two hypothetical etchants but may differ from the results expected with actual silicon etchants.

When using the Eshape model, there are three different corner types that must be considered:

Convex corners: If the original corner is convex then the resultant corner is the Esection which lies within the two lines which enclose the origin (see Figure 4, corner a).

Concave corners: If the original corner is concave then the resultant corner is the Esection which lies in the quadrant opposite the two lines which enclose the origin (see Figure 4, corner b).

Static corners: If there are no Esections in the appropriate area, the corner remains a sharp corner. The corner is located at the intersection of the two lines and its trajectory is along the radius from the origin to the intersection (see Figure 4, corner c).

Figure 6 shows a further example of the Eshape method.

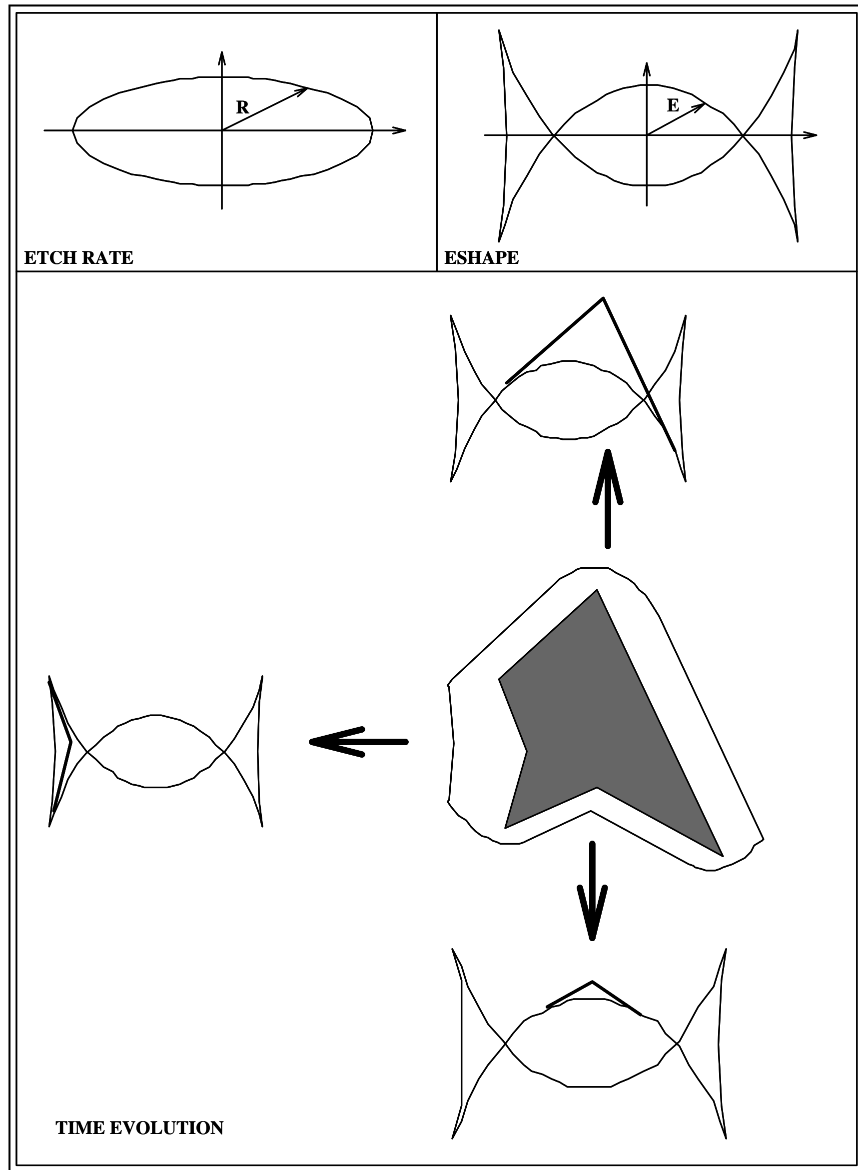

Figure 6: Summary of Eshape analysis: The etch rate is first transformed into an Eshape diagram. Then each corner is tangent-matched to the Eshape, and the appropriate Esection is extracted. The initial mask (shaded region) evolves to the surrounding curve. Convex corners use interior Esections, while concave corners use exterior Esections. The three corners shown are, starting at the top in counterclockwise order, convex, concave, and concave.

2.5 Time Evolution

A polygon evolves in the following manner: The etched shape at any time is formed by connecting each corner determined by the method above to its neighboring corners as shown in Figure 4. At each corner the extracted Esection is scaled (magnified) by the time. However as time increases, corners commonly intersect (see for example corners d and e in Figure 4) and some faces may disappear. The segments of corner sections that lie beyond the intersection of two corner sections do not appear in the final shape. Determination of the etched shape involves finding all such intersections, or cusps, and removing the non-physical segments.

The finding of such intersections has been extensively studied in the field of computer aided geometric design. Specifically, the etching process can be viewed as the generation of an offset curve with an orientation-dependent offset distance. Such offset curves [9] appear in applications such as numerically controlled machining.

In addition, new corners may appear and new Esections may have to be inserted when through-cut occurs (for example when two separate polygons merge into one larger polygon). After these new Esections have been added, the analysis proceeds as before.

3 Limit Shape

If the initial polygon is closed, then the corner angles must cover the range 0 to 360 degrees at least once. Therefore all parts of the Eshape are present in the etched shape, but each section is translated from the origin by the initial corner positions. As time goes to infinity, this initial translation becomes negligible compared to the size of the Esections, and the shape converges to Esections all centered at the origin. We define this to be the Eshape. Using the rules for intersections stated above we see that the etched shape at large time converges to the interior of the Eshape, termed the limit shape.

4 Time Scaling

Given two initial polygons where the second polygon is a scaled version of the first:

$$\{poly_2\} = \{poly_1\} * k \tag{9}$$

From Equation 6 ,

$$(C_{i_j}(t))_1 = \{P_i \ + t \ * \ E(\theta_{ij})\} \tag{10}$$

$$(C_{i_j}(t))_2 = \{P_i * k \ + t \ * \ E(\theta_{ij})\} \tag{11}$$

therefore $(C_{i_j}(k * t))_2 = k * (C_{i_j}(t))_1$ and

$$S_2(k * t) = k * S_1(t) \tag{12}$$

Thus, if a second polygonal mask twice as big as a first is etched, the shape of the second at time $2t$ is the shape of the first at time t, enlarged by a factor of two.

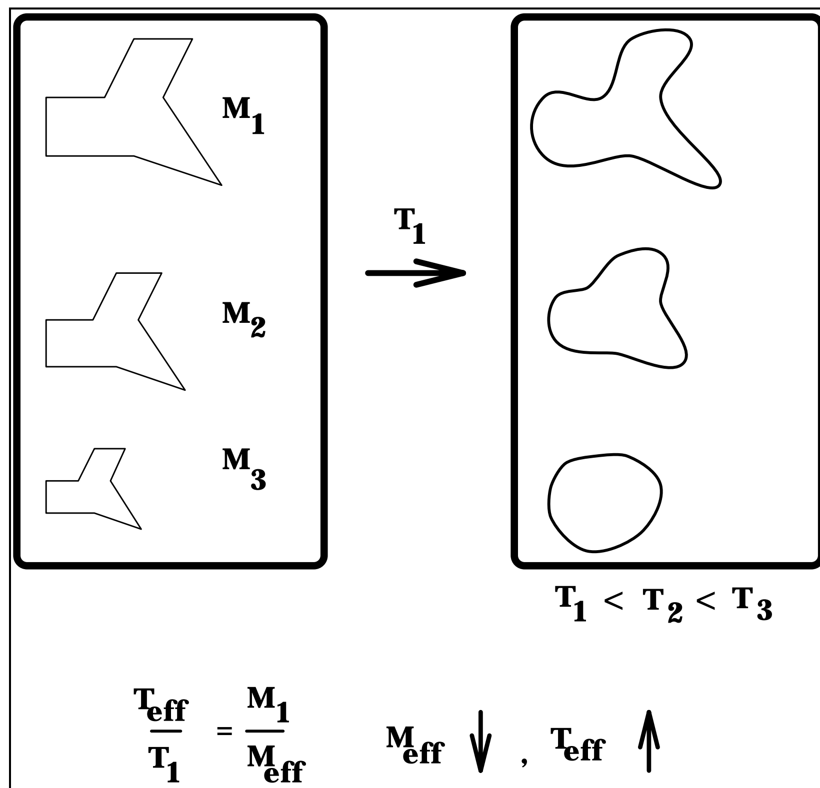

Figure 7: Time evolution of a shape in a single etch. The initial mask on left is repeated at different scales. The output shapes are on the right. The effective etch time is inversely proportional to scale.

Time scaling has a very important consequence: if several scaled versions of a mask are placed on a wafer and that wafer is etched for one value of time, then each of the evolved shapes will present a scaled version of the output shape at *different* values of time (see Figure 7). The smaller masks will represent the evolved shapes at larger time, with the effective time going as the inverse of the scale. This allows the entire time history of a shape to be etched in one experiment. This result has been verified by simulation and experiment.

5 Design Inversion

The most general and most powerful form of design inversion is: given a desired final etched shape and a particular etchant, what initial mask is necessary to produce the desired output? This is a very difficult problem to solve in general and there are some shapes for which it is impossible to design an input mask, however it may be possible to closely approximate the desired shape. For example in EDP or KOH etching, a diamond shaped hole tends to evolve into a octagonal shape (see

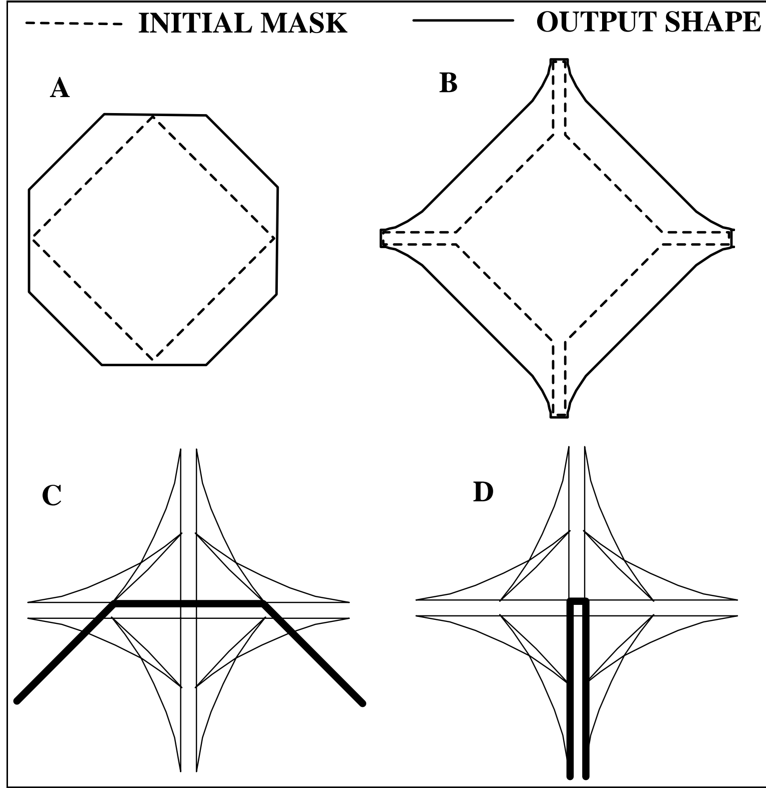

Figure 8: EDP or KOH etching: (A) diamond mask evolves to octagon. (B) modified diamond evolves to approximate diamond. (C) Eshape for (A). (D) Eshape for (B).

Figure 8A). If we desire a diamond we can approximate it by using the initial mask shown in (see Figure 8B).

This shape evolves into something which more closely resembles a diamond. The reason is immediately clear if we examine the Eshape. Consider the top corner: The first mask has a corner defined by the thick line (see Figure 8C). The second mask because of different tangent matching conditions, has a much sharper outline (see Figure 8D). This particular example has also been verified experimentally.

Another type of inversion is as follows: Given a desired output shape, what type of etchant is needed to etch this shape? Since the tangent of the Eshape is perpendicular to the rate, the normal of the Eshape is parallel to the rate and thus the inversion formula is given by

$$R(\theta) = (\vec{E} \cdot \hat{E}_{\perp})\hat{E}_{\perp} \tag{13}$$

where $\hat{E}_{\perp}$ is the unit normal of the Eshape.

To verify this capability, the Eshapes shown earlier were inverted and the original etch rate diagrams were obtained. This process is independent of desired output and because of the limit shape theorem is also independent of initial mask. Of

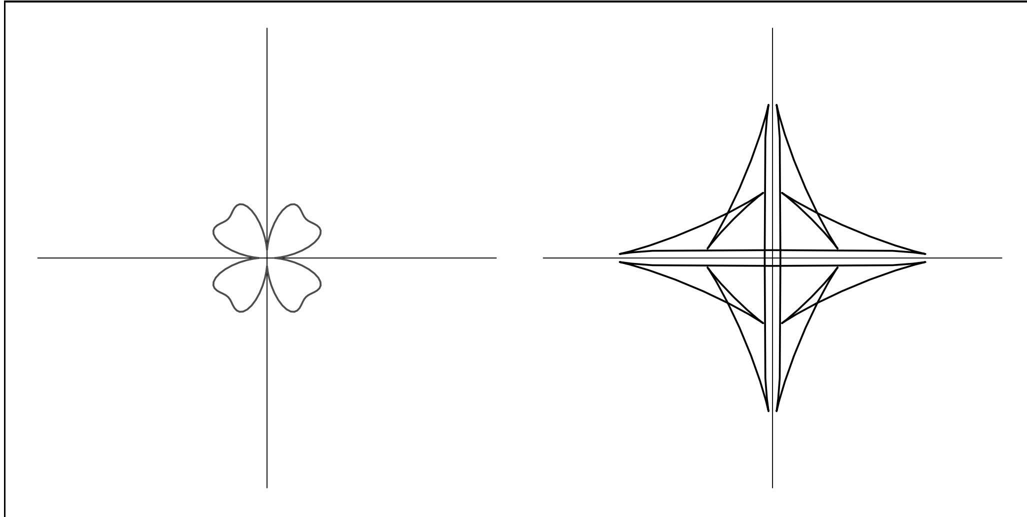

Figure 9: Etch rate diagram for (100) silicon in KOH and associated Eshape.

course this second form of inversion is limited by our ability to tailor the behavior of etchants. Nevertheless it provides information on the desired etchant behavior for any desired output specification.

6 Comparison with Experiment

6.1 Test patterns

A two dimensional model was used to model the surface outline of etched shapes. Tests were performed with both KOH and EDP, and although only the KOH results are presented here, the results from both etchants agreed with experiments. Samples were etched from one to two hours in a reflux system with temperature feedback. The temperatures for the KOH and EDP were 60 and 95 degrees Celcius respectively. In both cases the masking layer was silicon dioxide (approximately 0.8 microns in thickness).

The etch rate diagram in Figure 1 was used to generate the Eshape shown in Figure 9.

A test pattern was designed to verify different aspects of the model. The pattern included squares, circles, diamonds, and crosses of various sizes. In addition, both positive (holes) and negative (pegs) images were used. The Eshape of Figure 9 was use to generate the predicted shapes of Figure 10B. The model shows very good agreement with experiment as shown in Figure 11A. Note that both the pegs and the holes are accurately rendered as are both the convex and concave corners. In general it was found that the ability to predict output shapes is most limited by rate diagrams. Given that the Eshape model is a linear model, the error between the output shapes and the predicted results is on the order of the error between the

actual etch rate and the etch rate used by the model.

Figure 11B shows another etch of half the duration of Figure 11 A. Comparison of the two figures confirms that the time scaling rule is valid.

6.2 Spoke patterns

One way to experimentally obtain the etch rate as a function of orientation is to etch a bicycle spoke pattern constisting of many radial wedges (see Figure 12 A).

Simple geometry shows that for N spokes each centered about angle θ_i, the pattern P formed is given by:

$$P_i = \frac{t}{\sin\frac{\pi}{2N}} * \frac{1}{2} * \left[R\left(\theta_i + \frac{\pi}{2} * (1 + \frac{1}{N})\right) + R\left(\theta_i - \frac{\pi}{2} * (1 + \frac{1}{N})\right)\right] \quad (14)$$

where P_i is the radial position of the spoke at angle θ_i. This formulation illustrates four phenomena: (1) the pattern grows linearly in time; (2) the etch rate is magnified: as N increases, the effective etch rate increases; (3) the etch rate is averaged over the width of the spoke; (4) the pattern depends on the rates perpendicular to the spokes;

For etchants that have four-fold symmetry and for the number of spokes N large, the formulation reduces to:

$$P_i = \frac{2N}{\pi} * [R(\theta_i)] \quad (15)$$

Figure 12 B shows the Eshape simulation of the etching of the spoke pattern. Compare this both with Figure 1 and Figure 12 C & D. Figure 12 C & D show experimental etches in both EDP and KOH. The experimental patterns suffer from lithography problems at the center where all lines meet and the lithography resolution is exceeded. However, these problems may be minimized by increasing the size of the pattern which reduces the relative effect of the center region.

Finally a comparison of an enlargement of the wide ends of the spokes (Figure 12 C & D) to the simulation of this region (Figure 12 B) shows good agreement in modeling the etch rate pattern as well as the changing shape of the spoke ends.

7 Extension to Three Dimensions

7.1 Exact solution

The extension from two dimensions to three dimensions can be very complicated [4, 6]. Many different geometries can arise and have to be considered individually. Because of its intuitive nature, the extension of the Eshape method introduced above allows us to observe which corner types are possible, and to classify those types by inspection.

In three dimensions, consider a vector [x,y,z]. As in two dimensions we have a reference frame and a rotated frame. The rotated frame is located at some angle ϕ from the z axis and rotated from the x axis by an angle θ.

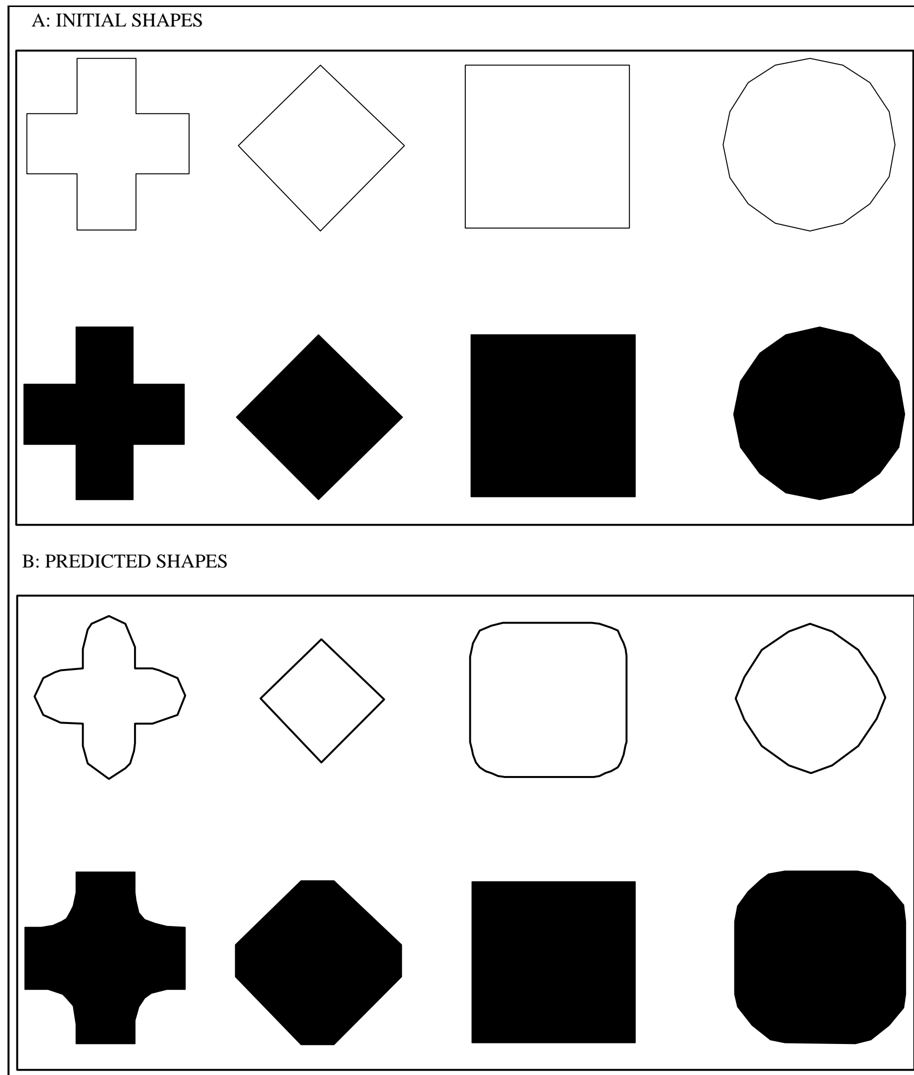

Figure 10: (A) Initial mask shapes; the squares are 0.8 mm across. (B) Predicted shapes derived from Figure 9. Compare with Figure 11. In both A and B, The top row of figures represents “pegs” while the bottom row represents “holes”.

photo here

Figure 11: (A) (100) silicon etched with KOH at 60°C for two hours. The largest square is 0.8 mm across. (B) (100) silicon etched with KOH at 60°C for one hour. Compare any shape in this figure with the corresponding shape in Figure 11 A. In both A and B, The top row of figures represents “pegs” while the bottom row represents “holes”.

photo here

Figure 12: (A) Initial spoke pattern. (B) Simulated etch using Eshape method with KOH etchant. Compare with Figure 1. (C) Spoke pattern etched in KOH. (D) Spoke pattern etch in EDP. Both patterns are approximately 1.5 centimeters across and both were etched for several hours. Note that the end regions on the simulations agree with the observed experiments.

Repeating the derivations for Equations 1 through 4 in three dimensions we obtain (compare with Equation 5):

$$\vec{E}(\theta,\phi,t) = \vec{C}_m + \left[R(\theta,\phi), \frac{\partial R(\theta,\phi)}{\partial \theta} * \frac{1}{\sin\phi}, \frac{\partial R(\theta,\phi)}{\partial \phi}\right] ROT_{\theta\phi} * t \qquad (16)$$

or

$$\vec{E}(\theta,\phi,t) = \vec{C}_m + R\ R_{\perp} \begin{bmatrix} 1 & 0 & 0 \\ 0 & -1 & 0 \\ 0 & 0 & -1 \end{bmatrix} ROT_{\theta\phi} * t \qquad (17)$$

Here:

$$ROT_{\theta\phi} = \begin{bmatrix} \sin\theta & 0 & -\cos\theta \\ 0 & 1 & 0 \\ \cos\theta & 0 & \sin\theta \end{bmatrix} \begin{bmatrix} \cos\phi & \sin\phi & 0 \\ -\sin\phi & \cos\phi & 0 \\ 0 & 0 & 1 \end{bmatrix} \qquad (18)$$

and $R_{\perp}$ is the local normal of $R(\theta,\phi)$ in spherical coordinates.

Hypothetical three dimensional etch rate diagrams have been formulated (since full 3-D etch rate information is not available in the literature) and the corresponding three dimensional Eshapes have been constructed using Equation 16.

The results for limit shapes and time scaling can also be extended to three dimensions.

7.2 Approximate three dimensional solution

Three dimensional etch simulation using the method described above can become quite complex, however, in many common situations an approximation is sufficient. Rather than examining the three dimensional evolution of corners, we can use the two dimensional outline (as a function of time) to simulate the three dimensional evolution of the edges which make up the shape. Two assumptions are necessary: (1) the etching is anisotropic, thus the cross section of any edge perpendicular to the (100) plane is a straight line inclined at some angle; (2) the depth is shallow, such that three dimensional corners do not intersect.

The shape is given by the two dimensional outline extended into the (100) plane at the appropriate angles. In order to calculate this, the inclination of planes (with respect to the z axis) as a function of orientation within the (100) plane must be obtained. This may be done from the spoke pattern described earlier.

EDP and KOH have similar etch rate diagrams in the (100) plane but they differ out of the (100) plane. Both produce 54.7 degree z-inclined planes for lines inclined at 0 or 90 degrees in the (100) plane. However, for planes inclined 45 degrees in the (100) plane, EDP produces a z-incline of 45 degrees while KOH produces vertical walls (90 degrees). Using this data and intermediate values, we can add to the two dimensional outline and produce three dimensional images. This was done for the experimental test patterns as shown in Figure 13 A. The results agree very well with the data.

The three dimensional representation allows us to view the shape from any direction we choose as shown in Figure 13 B.

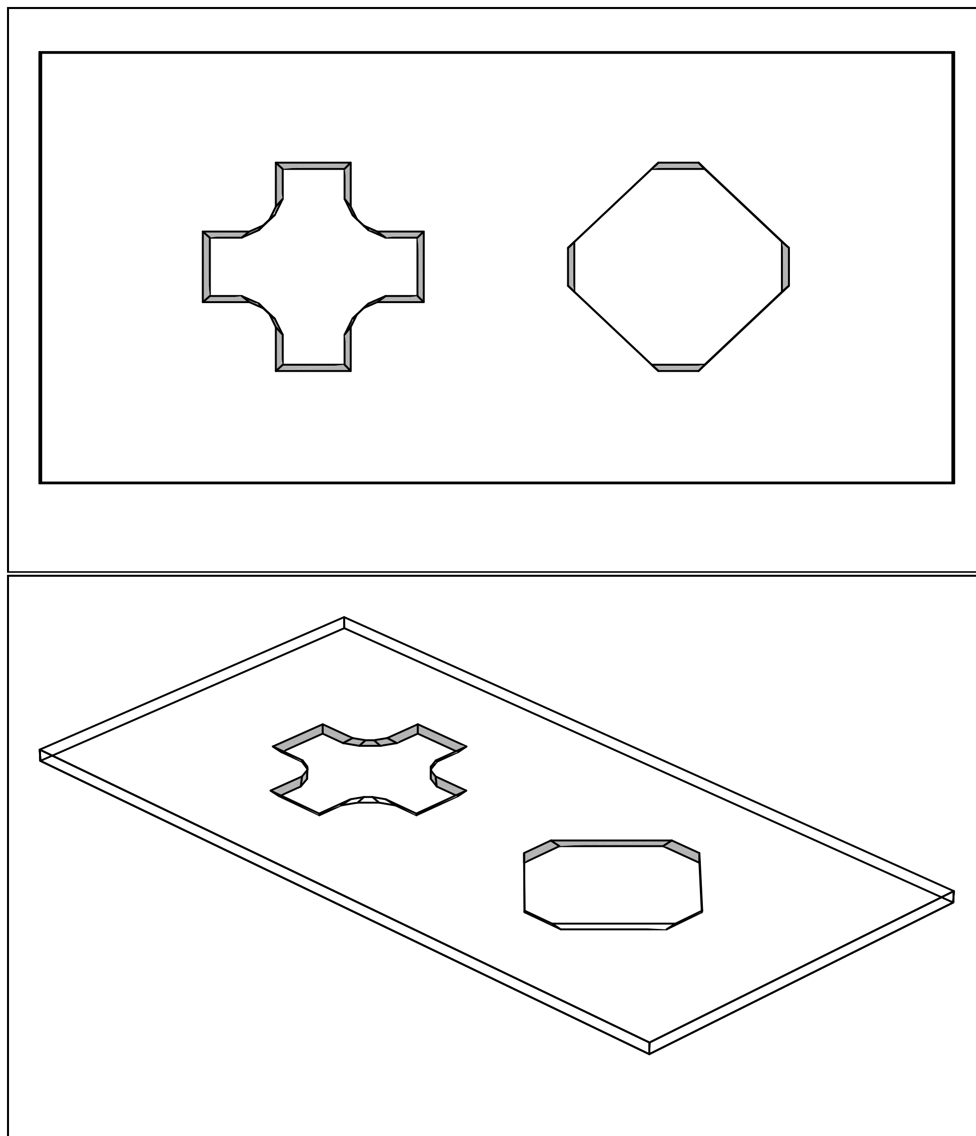

Figure 13: Cross and diamond shaped holes. (A: top) KOH etch simulation extension to three dimensions (B: bottom) View from an oblique angle. Compare with Figure 11.

8 Summary

Several models for analyzing MEMS exist and accurately model the future output shape given the initial conditions [4, 6, 7, 10]. The Eshape model also accurately predicts the output shapes, but offers some additional advantages. It provides a simple mathematical description of the etching process as well as a framework for inverting the design process to determining the required input mask for a desired output shape. Thus it is closer to CAD (Computer Aided Design) than to CAE (Computer Aided Analysis). The disadvantages of the Eshape model are shared by many other models. For example, a model is only as good as the etch rate information that is available. Additionally, when two or more etched shapes intersect to form new shapes, more detailed global calculations are required.

We have presented a new method for modeling the time development of emergent faces in crystal etching. This modeling is fundamental to MEMS fabrication simulations and design. The two dimensional Eshape method was presented, which is both intuitive and easy to implement manually or by computer. The concepts of equilibrium sections, equilibrium shapes, limit shapes, and time scaling were introduced. The predictions of the model agreed well with experiments performed with KOH and EDP. The Eshape etch model presented here is a first step in developing the ability to represent and manipulate complex (mechanical) shapes to be fabricated in silicon, and in developing comprehensive MEMS design methods which we hope will approach the level of development and automaticity in VLSI design.

Acknowledgments

The authors wish to gratefully acknowledge Professor Y.C. Tai for the use of his facilities and many helpful discussions. This material is based upon work supported, in part, by the National Science Foundation under Grant No. ECS-9023646. Any opinions, findings, conclusions or recommendations expressed in this publication are those of the authors and do not necessarily reflect the views of the sponsor.

References

[1] C. Mead and L. Conway. *Introduction to VLSI Systems.* Addison-Wesley Publishing Company, Reading, Massachusetts, 1980.

[2] U. Schnakenberg, W. Benecke, and B. Lochel. NH4 OH - based etchants for silicon micromachining. *Sensors and Actuators*, A21-A23:1031–1035, 1990.

[3] H. Seidel, L. Csepregi, A. Heuberger, and H. Baumgartel. Anisotropic etching of crystaline silicon in alkaline solutions. *J. Electrochem. Soc.*, 137:3613–3631, 1990.

[4] C. H. Sequin. Computer simulation of anisotropic crystal etching. In *Transducers '91*, pages 801–806, San Francisco, CA, USA, 1991.

[5] R.J. Jaccodine. Use of modified free energy theorems to predict equilibrium growing and etching shapes. *J. Appl. Phys.*, 33(8):2643–2647, August 1962.

[6] G. DeLapierre. Anisotropic crystal etching: A simulation program. *Sensors and Actuators*, 31:267–274, 1992.

[7] R. A. Buser and N. F. de Rooij. ASEP: A CAD program for silicon anisotropic etching. *Sensors and Actuators*, 28:71–78, 1991.

[8] George H. Martin. *Kinematics and Dynamics of Machines.* McGraw-Hill, New York, 1982.

[9] W. Tiller and E.G. Hanson. Offsets of two-dimensional profiles. *IEEE Comput. Graphics Appl.*, 4:36–46, 1984.

[10] F. C. Frank and M. B. Ives. Orientation-dependent dissolution of Germanium. *J. Appl. Phys.*, 31(11):1996–1999, November 1960.